

**A Holocene dinocyst record of a two-step transformation of the
Neoeuxinian brackish water lake into the Black Sea**

Fabienne Marret^{1*}, Peta Mudie², Ali Aksu³, Richard N. Hiscott³

¹Department of Geography, University of Liverpool, Liverpool, L69 7ZT, UK;
f.marret@liv.ac.uk

²Geological Survey Canada Atlantic, Dartmouth, Nova Scotia B2Y 4A2,
Canada; pmudie@nrcan.gc.ca

³Department Earth Sciences, Memorial University of Newfoundland, St. John's,
Newfoundland, A1B 3X5, Canada; aaksu@esd.mun.ca; rickh@esd.mun.ca

*corresponding author; Tel. +44 (0)151 794 28 48; Fax +44 (0)151 794 2866

Abstract

An exceptionally high-resolution and species-rich dinoflagellate cyst record from core M02-45 collected from the southwestern Black Sea shelf provides strong evidence of a gradual reconnection between the Black (BS) and Mediterranean (MS) seas at the beginning of the Holocene. Two main assemblages, one dominated by brackish species, *Spiniferites cruciformis* and *Pyxidinosia psilata*, and freshwater algae, and a subsequent one, characterised by euryhaline species (*Lingulodinium machaerophorum*, *Brigantedinium* spp., *Protoperidinium ponticum*), document a progressive change in sea-surface conditions from low saline (~7–12 psu) to present-day conditions. A first major pulse of marine waters is recorded at around 8.46 ka BP, with a maximum of *L. machaerophorum*. The occurrence of this species from the bottom of the core, dated at 9.3 ka BP, supports the hypothesis that water levels were already high on the southwestern shelf by that time. Fully present-day conditions are recorded at around 5.6 ka BP, when brackish species and morphotypes of *Spiniferites belerius*, *Spiniferites bentorii* and *L. machaerophorum* disappeared. Arrivals of Mediterranean species (*Operculodinium centrocarpum* and *Spiniferites mirabilis*) are observed simultaneously in the southwest and southeast region of the BS at around 7 ka BP. Despite a different protocol for palynomorph preparation and presentation of data, previous studies from the northern shelf also document the arrival of euryhaline species at 7 ka BP, and marine influence prior to that time. The history of harmful algal blooms (HABS) shows a correlation with warmer mid-Holocene temperatures, followed by a succession of introductions possibly associated with early Greek exploration, then merchant shipping.

Keywords: Dinocysts, Black Sea shelf, paleosalinity, brackish, morphotypes; harmful algae

1. Introduction

Over the last few years, the timing of, and the conditions in effect during the Holocene transition of the Black Sea from freshwater-brackish to marine have been the subject of wide debate, leading to the recent publication of the book “The Black Sea Flood Question” (Yanko-Hombach *et al.*, 2007). The proposed hypothesis of Ryan *et al.* (2003) that a catastrophic flood took place at around 8.4 ka BP when the Black Sea Level (BSL) was at -95m has been challenged by Aksu *et al.* (2002a, b) and Hiscott *et al.* (2002) (see Hiscott *et al.*, 2007 and in press, for more detail) with their *Outflow Hypothesis*. Multiproxy studies based on sedimentology, geochemistry and micropalaeontology document major changes at the beginning of the Holocene, but the timing and extent of these events are not in agreement with the Ryan *et al.* (2003) hypothesis, reinforced in Ryan (2007), with the exception of the recognition by both research groups of a significant marine incursion at around 8.4 ka BP (~9.4 cal ka BP; Major *et al.*, 2006).

Amongst these micropaleontological studies, organic-walled dinoflagellate cyst records have provided some significant evidence regarding the Black Sea surface water salinity prior to and after its connection to the Marmara Sea (Mudie *et al.*, 2001, 2002). Indeed, after the pioneering work of Wall *et al.* (1973) on Holocene dinocyst records in the Black Sea, a number of studies have been completed, in particular, in the southwestern and northwestern region of the Black Sea (Table 1, Fig. 1). These studies all document the occurrence of two to three successive dinoflagellate cyst (=dinocyst) assemblages, showing, for the early part of the Holocene, the dominance of the quasi-endemic *Spiniferites cruciformis*-*Pyxidinosia psilata* association, followed by the dominance of cosmopolitan euryhaline species such as *Lingulodinium machaerophorum* accompanied by Mediterranean-related *Spiniferites* and *Operculodinium* species, and near the top of the Holocene, an increase in heterotrophic protoperidinioid cysts.

The succession of these dinocyst associations is very significant for establishing the timing of the Mediterranean water incursions into the Black Sea at the beginning of the Holocene. Indeed, Mudie *et al.* (2004) demonstrate water exchange between the Marmara and the Black Seas around 9.5 ka BP, based on eight cores collected in the Marmara Sea, the southeastern Black Sea basins and the southwestern Black Sea shelf. More recently, the compilation of dinocyst records from the deep western part of the Black Sea (Atanassova, 2005) suggests that the inflow of Mediterranean waters occurred only later, around 7.1–7.5 ka BP, although there is some indication from these data that a marine influence was present at the beginning of the Holocene. Indeed, Filipova-Marinova (2007) points out the occurrence of single cysts of *L. machaerophorum* at around 9.6 ka BP in deep-sea sediments off the Bulgarian shelf.

In addition to the importance of organic-walled dinocysts as markers of surface water salinity (top ~50–100m), recent studies have begun to establish the importance of certain cyst species as markers of excess eutrophication in polluted marine waters (e.g. Dale *et al.*, 1999; Matsuoka, 1999; Matsuoka *et al.*, 2003; Mudie *et al.*, 2004) and as proxies for tracing the history of red tides and harmful algal blooms (HABs). The eutrophication in the Black Sea over the past 30 years has been accompanied by an increase in massive outbreaks of the calcareous-forming dinocyst *Scrippsiella trochoidea*, in addition to the white tides caused by the coccolith *Emiliana huxleyi* (Eker-Develi and Kideys, 2003; Oğuz and Merico, 2006). Some previous studies have attempted to outline this history of dinocyst HABS for the Black Sea (Mudie *et al.*, 2004, in press).

However, with the exception of a few samples from an 11 m-long piston core 1474P studied by Wall *et al.* (1973), and dated from 8.6–22.83 ka BP, most of the past records shown in Figure 1 are based on short cores (i.e., 60–250 cm long). These cores provide only very low resolution records, on the order of millennia in the Black Sea to centuries in Marmara Sea. Furthermore, a different protocol for sample

preparation for dinocyst analysis may explain the low dinocyst species diversity documented by Atanassova (2005) and by Filipova-Marinova (2006), as their pollen preparation followed the acetolysis method (Faegri and Iversen, 1989) that has been recognised as responsible for degrading or destroying protoperidinoïd cysts sensitive to oxidation (Dale, 1976; Marret, 1993; Head, 1996; Hopkins and McCarthy, 2002). Acetolysis treatment also darkens cysts and makes them more difficult to distinguish from reworked Pleistocene dinocysts (see discussion by Ravazzi, 2006). We use only acid digestion and sieving for cyst preparation, and we do not use the oxidant KOH that also damages delicate cysts.

We present here a new record of organic-walled dinocyst assemblages with decadal to centennial resolution, from a 950 cm-long core M02-45 collected at a water depth of 69 m from the southwestern shelf of the Black Sea (Fig. 2). Several radiocarbon dates (discussed below) indicate that the core covers the last 9.3 ka, with only one hiatus at 270 cm, spanning ~4.5–2.5 ka (Hiscott *et al.*, in press). The sampling resolution for this core is multi-decadal, thereby reducing the possibility that a major catastrophic event could be missed. This high resolution dinocyst record is discussed here in detail in order to further evaluate the validity of the catastrophic flood hypothesis proposed by Ryan *et al.* (1997, 2003) and Ryan (2007) *versus* the gradual drowning or outflow hypothesis of Aksu *et al.* (2002b) and Hiscott *et al.* (2007). We further compare the Black Sea shelf dinocyst assemblages with the recent record of dinocysts from Central Asian seas (Marret *et al.*, 2004) in order to refine the salinity ranges of 3–12 psu (practical salinity unit) previously assigned to the early Holocene cyst assemblages by various workers (Wall *et al.*, 1973; Mudie *et al.*, 2001, 2004, Filipova-Marinova, 2007).

2. Regional setting

2.1. Oceanography

The surface water circulation in the Black Sea is dominated by two large central cyclonic gyres (eastern and western gyres) and several smaller, anticyclonic coastal eddies (Öguz, 1993). The narrow (<75 km-wide) counterclockwise-rotating peripheral Rim Current separates the cyclonic gyres in the basins from the anticyclonic coastal eddies. This current flows eastward along the Anatolian coast with velocities of $\sim 20 \text{ cm s}^{-1}$ and dominates the surface circulation across the narrow continental shelves. The weaker Bosphorus and Sakarya anticyclonic eddies are situated west and east of the Strait of Bosphorus, respectively, and are confined to the coastal regions.

Three distinct water masses are recognised: a low salinity (17–18 psu), well ventilated surface water mass showing seasonably variable temperatures occupies the upper 50–90 m, an intermediate suboxic water mass (Cold Intermediate Water) occupies depths ranging from 50–100 m, and a high salinity, anoxic water mass occupies water depths below ~ 200 m (e.g. Murray, 1991). The water exchange between the Black Sea and the eastern Mediterranean Sea occurs through the Straits of Bosphorus and Dardanelles as a two-layer flow (Latif *et al.*, 1992). The cooler (5–15°C) and lower salinity (17–20 psu) surface layer originates from the Black Sea, and flows south/southwest across the Straits of Bosphorus and Dardanelles with velocities of $10\text{--}30 \text{ cm s}^{-1}$. The warmer (15–20°C) and high-salinity (38–39 psu) Mediterranean water mass flows northward across the Strait of Bosphorus with velocities of $5\text{--}15 \text{ cm s}^{-1}$, and penetrates the Black Sea where it constitutes the bottom water mass below the 100–200 m-thick surface layer (Özsoy *et al.*, 1995; Polat and Tuğrul, 1996).

Today there is a net export of $\sim 300 \text{ km}^3 \text{ yr}^{-1}$ of water from the Black Sea into the Aegean Sea across the Straits of Bosphorus and Dardanelles (Özsoy *et al.*, 1995). This outflow results from excess precipitation over the Black Sea ($\sim 300 \text{ km}^3 \text{ yr}^{-1}$) and fresh-water input by large rivers ($\sim 350 \text{ km}^3 \text{ yr}^{-1}$), which together exceed

evaporation ($\sim 350 \text{ km}^3 \text{ yr}^{-1}$) in the region. The Danube, Dniester, Dnieper, Southern Bug and Don Rivers drain $\sim 20\%$ of central and eastern Europe ($\sim 2 \text{ million km}^2$), and are the major sources of fresh water entering the Black Sea (UNESCO, 1969, 1993). The fresh-water inflow into the Black Sea shows large seasonal variations, with peak river discharges occurring during April and May. The narrow constriction at the Strait of Bosphorus forces the level of the Black Sea to fluctuate in perfect synchronicity with the interannual and seasonal variations of fresh water discharge into the basin, with a range of $\sim 50 \text{ cm}$ measured at various monitoring stations over the last century (Özsoy *et al.*, 1995, 1996).

2.2. Physiography

The southwestern Black Sea shelf is a generally flat, gently north-dipping platform dissected by a prominent channel (Bosphorus Channel) which connects the Strait of Bosphorus to the Bosphorus Canyon (Fig. 1). The channel is 200–500 m wide and 10–25 m deep and separates the shelf region into a 10–17 km-wide eastern shelf and a 25–35 km-wide western segment. The shelf-slope break in both areas occurs at $\sim 115\text{--}120 \text{ m}$ water depth, with $5^\circ\text{--}9^\circ$ slopes leading to the floor of the Black Sea basin at $\sim 2200 \text{ m}$, also known as the Euxine Abyssal Plain (Fig. 1). The slope is dissected by numerous submarine canyons and gullies. A prominent channel network that is still active today has been created by the saline inflow from the Mediterranean Sea where it enters the Black Sea as a quasi-continuously-flowing density current (Di Lorio and Yüce, 1999; Hiscott *et al.*, 2006). This saline-inflow channel lies west of the Bosphorus Canyon.

2.3. Seismic stratigraphy of the SW Black Sea shelf

A tight grid of ultra-high resolution Hunttec deep-tow-system (DTS) boomer profiles with an average line spacing of $\sim 2 \text{ km}$ has allowed detailed mapping of Holocene seismic units in the vicinity of coresite M02-45. These profiles were

collected using a deep-tow system with a 500 joule boomer source, recorded using both a single internal hydrophone and a 21-element 6 m-long Benthos hydrophone streamer. The profiles have a vertical resolution of 15–30 cm, and penetration of 50–100 m below the seabed. We have mapped three seismic units on the shelf (from oldest to youngest, 1B, 1C and 1D) (Fig. 2; Hiscott *et al.*, in press). These units correspond to seismic units 1B, 1C and 1D of Aksu *et al.* (2002a); their seismic unit 1A is only present at the shelf edge and consists of lowstand delta lobes. On the middle shelf, unit 1B directly overlies the post-lowstand transgressive unconformity, α (Fig. 2). Unit 1C overlies a widespread reflection called α_1 that is locally an erosional unconformity. Unit 1D overlies a second unconformity, α_2 , that is in most profiles an onlap surface (Fig. 2). At coresite M02-45, seismic data provide no evidence for an hiatus at α_1 , whereas α_2 is an onlap surface (Hiscott *et al.*, in press).

Seismic unit 1B consists of discontinuous, subtly mounded, moderately strong reflections above unconformity α , passing quickly upward into weaker but very continuous reflections (Fig. 2). This reflection configuration is characteristic of stratified muds, although the basal hummocky and more reflective deposits are likely more sand-prone. A structure-contour map of the α unconformity surface shows that deposition occurred in a semi-enclosed shelf depression which opened toward the north (Hiscott *et al.*, in press), indicating unrestricted communication between the middle shelf and the Black Sea basin. Khrischev and Georgiev (1991) mention a washout surface in the western Black Sea at the Pleistocene-Holocene boundary that corresponds to our unconformity α .

Seismic unit 1C has a distinctive acoustic character, consisting of moderately strong but highly discontinuous and “crinkly” reflections (Fig. 2). Elsewhere on the southwestern Black Sea shelf, it passes laterally into morphological mounds interpreted as mud volcanoes by Aksu *et al.* (2002a; their fig. 17). Near the coresite

M02-45, unit 1C has a sheet-like geometry with only gradual thickness changes. The top of this unit is marked by onlap in almost all seismic profiles (i.e., unconformity α_2).

In the vicinity of coresite M02-45, seismic unit 1D is very similar in reflection character and continuity to unit 1B (Fig. 2). Elsewhere on the shelf, it forms drift-like deposits around elevated mud volcanoes and shelf ridges, and contains many internal truncation surfaces attributed to variable shelf currents (Aksu *et al.*, 2002a, Hiscott *et al.*, in press).

3. Material and Methods

3.1 Chronology of core M02-45

The piston core (M02-45P) and its trigger-weight core (M02-45TWC) were collected at 41°41.17'N, 28°19.08'E. Radiocarbon dates (all uncalibrated and not corrected for the reservoir effect due to the uncertainty in the correction; see Major, 2002) in both cores (Table 2) indicate ~110 cm of core-top loss in the piston core (Hiscott *et al.*, in press). All depths in this paper are given relative to the seafloor at the coresite, with the result that the top of the piston core has been adjusted downward to a depth of 110 cm to account for the core-top loss. The composite succession obtained by splicing together records from the trigger-weight and piston cores is designated as core M02-45.

A plot of radiocarbon dates against depth indicates accumulation rates of ~360 cm/1000 yr from 605–950 cm depth, ~85 cm/1000 yr from 330–605 cm depth, and ~125 cm/1000 yr in the upper 268 cm of the composite core. The age discontinuity between 268 cm and 330 cm correlates with the approximate depth of α_2 – based on facies in the core, α_2 is correlated to a core depth of 270 cm. The youngest deposits beneath α_2 have an age of ~4.5 ka and the duration of the hiatus is ~2000 years. There is no apparent hiatus at α_1 , but correlation of the dated core to the seismic

data suggests an age of ~7500 yr BP. Farther east on the southern Black Sea shelf, Mart *et al.* (2006) identify an equivalent unconformity which is overlain by sediments younger than 4400 yr BP.

Unconformity α is believed to be at least 250 cm below the base of core M02-45 (Table 2). Based on accumulation rates, α is therefore inferred to be at least 700 years older than the deepest recovered sediments. This provides a minimum age of ~10 ka for α . The approximate ages of seismic units 1B, 1C and 1D are therefore 10–7.5 ka, 7.5–4.5 ka, and 2.5–0 ka, respectively.

3.2. Palynology

Cores M02-45T (trigger weight) and M02-45P (piston core) were sampled every 10 cm for palynological analysis. Samples were prepared as follows: about 5–10 cm³ (4–8 g dry weight) of sediment was successively attacked with cold hydrochloric acid (diluted at 10%) and cold hydrofluoric acid (40%) in order to remove the carbonate and silicate fractions. Prior to the acid treatments, an exotic marker (*Lycopodium clavatum*) was added in order to facilitate the estimation of the palynomorph concentration. The resulting organic fraction was then mixed with Calgon detergent to disaggregate the sediment, and sieved at 125 μ m and 10 μ m to remove the coarse particles and remaining fine silt-clay sized sediment. The organic residue was then mounted in glycerine gel stained with safranin.

When possible, 300 cysts were identified, enabling the representation of all species present in the sample; however, many samples have low cyst contents and a minimum count of 100 cysts was achieved on average. Calculation of relative abundances (percentages) is based on the total sum of dinocysts. The dinocyst zones were established according to the cluster analysis performed with CONISS (Grimm, 1987), in the TILIA software (Grimm, 1990–1993).

Taxonomy of organic-walled dinocysts follows that of Wall *et al.* (1973), Fensome *et al.* (1993) and Marret *et al.* (2004). *Brigantedinium* spp. include all round-brown specimens not identified at the species level due to poor orientation. *Spiniferites* spp. includes all *Spiniferites* taxa not identifiable at the species level; the same applies to the *Echinidinium* spp. group. Microreticulate cysts of *Gymnodinium* were systematically measured in order to discriminate between *Gymnodinium catenatum* and *G. nolleri*. The cyst size ranges between 27 and 36 μm , which falls into the overlap between large *G. nolleri* cysts and small *G. catenatum* cysts (Ellegaard and Moestrup, 1999; Bolch and Reynolds, 2002). This discrimination is particularly significant as *G. nolleri* is a non-toxic species whereas *G. catenatum* is toxic. However, the surface reticulation of the cyst body differs between these two species, in the region of the paracingulum, and close observation of the specimens suggests that they may belong to the *G. catenatum* group (Ellegaard, pers. com.).

Cysts of *Alexandrium* species were also identified based on reference slides of recent cysts of *Alexandrium tamarense*. These differ from the wrinkled-walled specimens of *Scrippsiella* (Head *et al.*, 2006) that were often identified as cysts of *A. tamarense*.

Specimens of *Lingulodinium machaerophorum* vary in morphology, from the *sensu stricto* specimen with long processes to very short and bulbous processes (Plate 1). Four groups of morphotypes were distinguished in order to observe any trend in the record in relation to changes in environmental conditions. *L. machaerophorum* var. A has longer than normal processes, with no conical bases and the wall surface of the cyst body is scabrate. Processes are also scabrate and thin. *L. machaerophorum* var. B has a majority of processes with bulbous tips with a normal length. *L. machaerophorum* var. C has acuminate and thin processes, half the normal size. The last group (*L. machaerophorum* s.p. (short processes)) consists of specimens with very short and bulbous, or sometimes spine-like processes.

In parallel with the dinocyst counts, freshwater algae, coenobia of *Pediastrum simplex*, *P. boryanum*, and *P. kawraiskyi*, *Botryococcus* sp. and *Concentricystes circulus*, were also counted routinely and their percentages are based on the dinocyst sum + freshwater algae sum. Acritarch-type specimens such as *Cymatiosphaera*, *Sigmopollis*, *Halodinium*, *Beringiella* and *Paleostomocystis* were also encountered, particularly in the upper half of the piston core and in the trigger weight core, but they were not routinely counted and they will be described in another paper.

3-3. Coccoliths

For coccolith studies, ~5 cc sediment was removed at 10 cm intervals from the core, and samples were wet sieved through a 63 μm screen. The <63 μm fractions were further wet sieved through a 20 μm cloth and the <2 μm fractions were separated out using centrifugation. Coccoliths were identified and counted in the 20–2 μm fractions using the taxonomic descriptions of Kleijne (1993) and Winter *et al.* (1994). Only the counts of *Emiliana huxleyi* are reported in Figure 4.

4. Results

A total of 32 organic-walled dinocyst species and distinctive morphotypes (excluding groups such as *Brigantedinium* spp., *Spiniferites* spp. and *Echinidinium* spp.) were identified (Table 3), and three dinocyst assemblage zones were recognised (Figs. 3 and 4) based on cluster analysis (CONISS in Tilia, Grimm, 1990–1993). Overall, the concentration and fluxes are relatively low (on average 12460 cyst/g and 1515 cyst/cm²·ka⁻¹ respectively) with the exception of one maximum (120,190 cysts/g and 13860 cyst/cm²·ka⁻¹) at around 350–360 cm (~5.45–5.36 ka BP) and two minor peaks at 710 cm (~8.6 ka BP) and 460 cm (~6.6 ka BP).

Dinocyst Zone 1 (core bottom to 485 cm; ~9.5–~7.0 ka BP) is characterised by the dominance of the brackish species *Spiniferites cruciformis* and *Pyxidinosia psilata*, accompanied by freshwater algae (*Pediastrum coenobia* and *Botryococcus*). At around 710 cm (~8.6 ka BP), these cyst species show an abrupt flux increase. Diversity is low overall, with only 10 taxa occurring, notably two protoperidinian taxa (*Brigantedinium* spp. and *Quinquecuspis* sp.) and *L. machaerophorum* s.s., a cosmopolitan euryhaline species. This latter species occurs in almost all samples (except in the sample from a depth of 890 cm, ~9.0 ka BP) always in low abundance except at a composite core depth of 640 cm (~8.46 ka BP) where it reaches a maximum of 26 %. Note that in this zone, concentrations are low and, on average, about 100 specimens were counted in each sample. However, a double peak of *P. psilata* and *S. cruciformis* fluxes is observed at 860 cm and 710 cm (8.8 and 8.6 ka BP respectively). Other marine taxa occur sporadically such as cysts of *Pentapharsodinium dalei*, *Echinidinium transparentum*, *Spiniferites belerius*, *Spiniferites bentorii*, as well a peak (41%) of *Brigantedinium* spp. at around 500 cm depth (7.2 ka BP).

Dinocyst Zone 2 (from 485 cm to 385 cm; ~7.0–5.7 ka BP) is dominated by *L. machaerophorum* s.s. and an increase of its morphotypes as well as *S. belerius* and *S. bentorii* and their morphotypes. *Spiniferites* specimens from this zone show a strong morphological gradient, from ovoid body shape to slightly cruciform (Plate 1). However, their main characteristic features enable them to be assigned to either *S. bentorii* or *S. belerius*. Concentrations and flux as well as diversity increase upward, on average. Cysts of *P. dalei* increase, whereas *S. cruciformis* and freshwater algae disappear and *P. psilata* shows a strong decline to less than 2%. This zone also is characterised by a low occurrence of cysts of *P. kofoidii*, a known heterotrophic marine species, as well as cysts of *P. dalei* and *D. caperatum*, both cosmopolitan in marine environments. Sporadic occurrences of *O. centrocarpum* and *S. mirabilis* are observed, always in low abundance.

Dinocyst Zone 3 (from 385 cm to the core top; 5.7–~0 ka BP) can be divided into two subzones: dinozone 3a (385–280cm; 5.7–4.5 ka BP) and dinozone 3b (280 cm to top; 2.5–~0 ka BP). The α_2 hiatus separates these subzones, so that no samples have ages between ~4.5 ka BP and ~2.5 ka BP. Dinozone 3a is dominated at ~80% by *L. machaerophorum* s.s. and morphotypes, and low abundance of *Brigantedinium* spp. and other protoperidinioid taxa. Concentrations and fluxes are at their maximum (up to 120,190 cysts/g and 13860 cyst/cm²·ka⁻¹ respectively). *P. psilata* only occurs sporadically, always in percentages lower than 0.5%. Dinozone 3b is still dominated by *L. machaerophorum* s.s., but with less abundance of its morphotypes. Mediterranean-related species such as *Operculodinium centrocarpum* and *Spiniferites mirabilis* have a 2 to 4% presence and diversity reaches its highest level within the whole sequence. Amongst the protoperidinian species, *Protoperidinium ponticum*, a species first described by Wall and Dale in Wall *et al.* (1973), also increases significantly, up to 12%, in samples with an age of around 0.7 ka BP. This taxon first appears in Zone 2, always in percentages lower than 1%. A few sporadic occurrence of *Pediastrum coenobia* are also observed. Zone 3 is also characterised by the low occurrence of microreticulate gymnodinoid cysts, assigned to the group *Gymnodinium catenatum/nolleri*. They appear at a depth of around 260 cm (2.3 ka BP) and are observed up to near the top of the core.

5- Discussion

5.1 First arrival of euryhaline species

Core M02-45 provides the first high-resolution record of dinocyst assemblage succession for most of the Holocene in the southwestern Black Sea. The decadal to centennial resolution enables us to time the arrival and disappearance of species

related to specific sea-surface conditions. Overall, this record is characterised by the succession of two major associations: the first one, composed of the stenohaline, brackish to freshwater taxa *S. cruciformis* and *P. psilata*, occurs from the bottom of the record to around 7.2 ka BP and is followed upward by an association composed of euryhaline, brackish to hypersaline species. However, the deepest occurrence of euryhaline species, such as *L. machaerophorum*, is at the bottom of the core and the oldest peak of abundance for this euryhaline species is at around 8.46 ka BP. It is known from laboratory experiments that *L. polyedrum*, the vegetative (thecate) stage of this dinocyst, does not grow when salinity is below 10 psu (Lewis and Hallett, 1997) and also does not occur in environments where salinity drops below 7 psu, as for instance in the Baltic Sea (Dale, 1996). Therefore, it must be assumed that sea-water conditions at the beginning of the Holocene in the Neoeuxinian lake were not freshwater but brackish, in the range between 7–12 psu, as also estimated by Mudie *et al.* (2001) using the oxygen isotopes of planktonic foraminifera that co-occurred with *S. cruciformis* in the Marmara Sea. Mudie *et al.* (2001; in press) have also reported a weak correlation (maximum $r=0.54$) between the occurrence of various morphotypes of *S. cruciformis* and salinity, with the most reduced processes being associated with higher salinities. In contrast, Kouli *et al.* (2001) have found *S. cruciformis* with expanded processes in a fresh water mountain lake of Greece.

New evidence of ecological affinities for *S. cruciformis* and *P. psilata* have been obtained from their occurrence in recent sediments of the Caspian Sea, where salinity is overall around 12–13 psu, except in the north basin near the Volga river discharge (Marret *et al.*, 2004). Morphotypes of *S. cruciformis* were also observed in the Caspian Sea study but the relationships between cyst shapes and salinity or other sea-surface parameters remains equivocal and awaits further laboratory experiments and/or more observations in the field. However, their occurrence in modern environments confirms that these species can tolerate a salinity range up to 12–13 psu. It must be noted that a few specimens endemic to the Caspian Sea such

as *Impagidinium caspiense* and *Caspidinium rugosum* were observed in core M02-45 at the base of the Holocene in the southwestern Black Sea (Fig. 3).

The upward passage from one association to the other does not show abrupt changes in the species composition but rather a gradual shift. The decline of the brackish species started from around 7.6 ka BP and their disappearance is observed at around 6.9 ka BP for *S. cruciformis* and 6.0 ka BP for *P. psilata*. Between the disappearance of *S. cruciformis* and the full dominance of *L. machaerophorum* that began at 5.6 ka BP, a relatively high number (6) and abundance of morphotypes of *L. machaerophorum*, *S. belerius* and *S. bentorii* are observed. These occurrences signify changes in sea-surface conditions that are probably related to salinity and/or density. We therefore attribute this morphological variability to a changing environment, from brackish to more marine conditions, over ~1500 years. A first major pulse of marine conditions at around 8.46 ka BP is consistent with the results of Major *et al.* (2006) who described a sharp transition in $\delta^{18}\text{O}$, $^{87}\text{Sr}/^{86}\text{Sr}$ and Sr/Ca records from the northern Black Sea shelf at around this time. This pulse also accords with the total sulphur and the $\delta^{34}\text{S}$ record in core M02-45 (Hiscott *et al.*, in press). A second significant change occurred at around 5.7 ka BP when all morphotypes disappeared and *L. machaerophorum* s.s. fully dominates the assemblages, accompanied by *S. belerius* and *S. bentorii*; minimal occurrences of other euryhaline species such as *S. mirabilis* and *O. centrocarpum* are observed from ~7 ka BP and ~6 ka BP respectively. In the southeastern Black Sea, these two species first occur around 7 ka BP (Mudie *et al.*, 2002).

The controversy regarding the *flood hypothesis* of Ryan *et al.* (2003) lies now in the rate at which the reconnection of the Black Sea with the Mediterranean Sea occurred. For Ryan *et al.* (2003) and Lericolais *et al.* (2007), the preservation of dune-shaped relief lying at -85 m and -100m indicates rapid transgression at around 8.4 ka BP and 7.4 ka BP, respectively. However, these young dates contradict the

sedimentological data from core M02-45 which demonstrate the presence of at least a few tens of meters of waters above the core site (now at -69m on the southwestern shelf) at 9.3 ka BP. Hiscott *et al.* (in press) have shown that there was an open connection between the core site and the open Black Sea basin at 9.3 ka BP based on the mapping of the α unconformity. Furthermore, the coherent dinocyst signal from north and southwestern shelves (Table 4), even though some records lack the same temporal resolution and species diversity, strongly supports the hypothesis that water levels were already relatively high at 9.3 ka BP. These data are also consistent with those of Glebov and Shel'ting (2007) based on extensive seismic surveys and geological investigations of the Russian Black Sea shelf.

5.2 Late Holocene and impact of ship transport

The history of red tides and harmful algal blooms (HABS) in the Black Sea has become important in recent years because of the explosive increase in various phytoplankton species from ~1970 to 1992 (Bodeneau, 1993; Gómez and Boicenco, 2004; Oğuz, 2005). This period of increased eutrophication and warming in the Black Sea, combined with overfishing (Daskalov, 2002), led to a trophic food chain collapse, with dinocysts almost replacing the diatoms, and culminating in the invasion of ctenophores (*Mnemiopsis leidyi*) after 1993. By 2004, 267 species and 54 genera of dinoflagellates were reported for the Black Sea, of which 26 regularly or periodically formed HABS. In Izmit Bay, a highly polluted bay in the eastern Marmara Sea, near the entrance to the Bosphorus Strait, Aktan (2005) also reported that fourteen toxic and harmful dinoflagellate species had invaded during the past 40 years.

Most of these HAB dinoflagellates do not produce thick-walled resting cysts, therefore they cannot be traced in the paleoceanographic records. However, it is possible to examine the history of the potentially toxic species *L. polyedrum*, *Protoceratium reticulatum*, *Gymnodinium catenatum/holleri* and *Alexandrium* spp.,

and the histories of the calcareous dinoflagellate *Scrippsiella trochoidea* and the coccolith *Emiliana huxleyii* that periodically form white tides in parts of the northern Mediterranean and Black Sea.

The high resolution dinocyst record for M02-45 (Fig. 3) clearly shows that large numbers of cysts of *L. polyedrum* and *P. reticulatum* were already present in the southwestern Black Sea by at least 6.2 ka BP. The first large sustained peak of *L. polyedrum* cysts (= *L. machaerophorum*) occurred during the Late Eneolithic period, from ~6–5 Ka BP, which is considered to be the warmest period in the Holocene climate record for the Black Sea (Cordova and Lehman, 2005). The first occurrences of *Emiliana huxleyii* and *G. catenatum/nolleri*, however, appear to be much later (2.5 ka), although the hiatus in core M02-45 prevents precise dating of their first arrivals.

Previously identified as *G. catenatum* in a long Holocene record in the NE North Atlantic (Thorsen *et al.*, 1995), these specimens are now considered as *G. nolleri*, implying that most identifications of such microreticulate cysts were mistaken. Studies of recent sediments in the North Atlantic suggest that *G. catenatum* only arrived in the 20th century (e.g. Bravo and Ramilo, 1999, Amorim *et al.*, 2001, 2006), in a similar way as in the Pacific Ocean *via* discharge of ballast water from large ships. Large ballast water tanks were not invented until 1857AD, when the *Rouen* was constructed with double-bottom tanks (Kemp, 1980). Nonetheless, discharge of ballast water was also suggested to explain the sudden appearance of the coccolithophorid *Emiliana huxleyii* in the Black Sea between 3450 and 3000 yr BP (Jones, 1993), about 1,000 years after the first Greek explorations by galleys such as *The Argo* of Jason and his Argonauts (Severin, 1985). The earliest known large vessels that might have transported cysts into the Black Sea were actually open galleys without ballast water containers but they undoubtedly accumulated bilge water swept aboard during storms in the Aegean. This bilge would later be bailed out into the Marmara and Black Seas and could be a means of introducing new dinoflagellate species. The Greek merchant galley *Kyrenia* that sank *ca.* 2300 yr BP

(Swiny and Katzev, 1973) was decked over the bow and stern, and was filled with over 400 shipping jars stacked in a narrow-based hull that would collect a large amount of bilge water. By the first century, 3-decked Roman merchant ships sailed the Mediterranean, transporting wine, oil, fish paste, salted fish and snails from Spain to Greece (Parker, 1973). It is therefore possible that viable dinocysts were transported with these fish and snail products if they were stored in sealed jars. Torr (1964) reports that the Roman ships of 50 AD required quantities of gravel, sand or stone ballast at the bottom of the hold, for steadying the ship. In this hold there was also “a mass of bilge-water, which needed constant bailing out by buckets or else by a machine consisting of an Archimedean screw worked by some sort of treadmill” (cf. Athaenaeos v.43 in Torr, 1984).

The appearance of *E. huxleyii* at around 3000 yr BP in the southern Black Sea also coincides with the appearance of large amounts of *Scrippsiellia trochoidea* (see Ross and Degens, 1974; Fig. 3d) in cores from off Sinope. But it is not surprising that later cyst introductions like *G. catenatum/nolleri* do not occur until 2200 yr BP when merchant ships were larger, with deep hulls filled with amphora containing olive oil and fish sauce from the Mediterranean and southern Black Sea for trade of fish and hides at ports like Olbia on the northern shore (King, 2004). The oldest preserved Black Sea ship that sank off Sinope 1610 yr +/- 40 yr BP (Ward and Ballard, 2004) provides an example of how Mediterranean water and sediment could have been accidentally dumped into the Black Sea.

The youngest HAB dinocyst appearance is the potentially toxic *Alexandrium*-type cyst at approximately 900 yr BP in M02-45, and a few of these cysts were also found in surface sediments of cores from the Marmara Sea (Mudie *et al.*, 2004). This time period corresponds to the end of the Byzantine era when Roman, Khazar, Norse and Bulgar trading was at its height in the Crimean-Azov region of the Black Sea (King, 2004).

6- Conclusions

The decadal to centennial dinoflagellate cyst record clearly highlights a succession of different water masses that are related to the connection between the Black and Mediterranean Seas. The data from this study particularly address the issue of the timing and the rate of MS flooding into the Black Sea at the beginning of the Holocene. The evidence from the successive dinocyst associations demonstrate that a major pulse of marine waters occurred around 8.5 ka BP although marine conditions were already present at the location of the core by 9.3 ka PB. The recent information about ecological affinities for *S. cruciformis* and *P. psilata* enable us to qualitatively reconstruct the past salinity of the Black Sea before the full connection with the Mediterranean waters, and confirms that the Neoeuxinian “Lake” was brackish, with a salinity range between 7 and 12 psu. The transition between the dominance of brackish species to fully euryhaline association is gradual, over about 1500 years, and is characterised by strong morphological variations of dinocyst species such as *S. belerius*, *S. cruciformis*, *S. bentorii* and *L. machaerophorum*.

In addition, this record has drawn attention to the first arrival of HAB-forming species in the Black Sea during the Holocene, although the hiatus prevents us from being able to exactly pinpoint the timing. Paleoceanography is a powerful tool for understanding the history of harmful algal blooms (HABs) and hence forecasting the direction of future outbreaks. The frequency of the HABs in the Black Sea is correlated with Global Warming over the past 30 years and it has been predicted that increased warming will accelerate this trend. This forecast is supported by the high resolution marine palynology records from M02-45 which show that very large blooms of *Lingulodinium polyedrum* cysts occurred during the thermal maximum from about 6,000–5,000 years ago, and that introduction of new HAB cysts has occurred over the past ~2,000 years.

The future establishment of larger databases of modern dinocyst assemblages from the Black Sea and adjacent seas (Caspian Sea, Azov Sea, and Marmara Sea) will enable us to develop a powerful tool to quantitatively reconstruct past sea-surface conditions

7- Acknowledgements

We thank the officers and crew of the RV Koca Piri Reis for invaluable assistance during a succession of successful cruises. Aksu, Hiscott and Mudie acknowledge funding and in-kind support from the Natural Sciences and Engineering Research Council of Canada, the Piri Reis Foundation, the Geological Survey of Canada, and the Vice-President (Research) of Memorial University of Newfoundland. We thank Helen Gillespie, Memorial University of Newfoundland for her assistance in the palynological sample preparations. We thank the Isotrace Laboratories, University of Toronto, for the C-14 dates. The authors are thankful to the M. Filipova-Marinova and an anonymous reviewer for their comments that helped to improve this manuscript.

References

Aksu, A. E., Hiscott, R. N., Kaminski, M. A., Mudie, P. J., Gillespie, H., Abrajano, T., Yaşar, D., 2002a. Last glacial-Holocene paleoceanography of the Black Sea and Marmara Sea: stable isotopic foraminiferal and coccolith evidence. *Marine Geology* 190(1-2), 119-149.

Aksu, A. E., Hiscott, R. N., Mudie, P. J., Rochon, A., Kaminski, M. A., Abrajano, T., Yaşar, D., 2002b. Persistent Holocene outflow from the Black Sea to the Eastern Mediterranean contradicts Noah's Flood hypothesis. *GSA Today* 12(4-9).

Aktan, Y., 2005. Toxic and harmful algal species in the Izmit Bay, Marmara Sea. *Harmful Algal News* 28, 6.

Amorim, A., Dale, B., Godinho, R., Brotas, V., 2001. *Gymnodinium catenatum*-like cysts (Dinophyceae) in recent sediments from the coast of Portugal. *Phycologia* 40(6), 572-582.

Amorim, A., Dale, B., 2006. Historical cyst record as evidence for the recent introduction of the dinoflagellate *Gymnodinium catenatum* in the north-eastern Atlantic. *African Journal of Marine Science* 28(2), 193.

Atanassova, J., Bozilova, E., 1992. Palynological investigation of marine sediments from the western sector of the Black Sea. *Proceedings of the Institute of Oceanology (Varna)*. 1, 97-103.

Atanassova, J., 1995. Dinoflagellate cysts from Late Quaternary and recent sediments of the Western Black Sea. *Annual of Sofia University "St. Kliment Ohridski", Faculty of Biology* 87(2), 17-28.

Atanassova, J., 2005. Palaeoecological setting of the western Black Sea area during the last 15 000 years. *The Holocene* 15(4), 576-584.

Bodeneau, N., 1993. Microalgal blooms in the Romanian area of the Black Sea and contemporary eutrophication conditions. In: Smayda, J., Shimizu, Y. (Eds), *Toxic Phytoplankton Blooms*. Elsevier Science, pp. 203-209.

Bolch, C. J. S., Reynolds, M. J., 2002. Species resolution and global distribution of microreticulate dinoflagellate cysts. *Journal of Plankton Research* 24(6), 565-578.

Bravo, I., Ramilo, I., 1999. Distribution of microreticulate dinoflagellate cysts from the Galician and Portuguese coast. *Scientia Marina* 63(1), 45-50.

Cordova, C. E., Lehman, P. H., 2005. Holocene environmental change in southwestern Crimea (Ukraine) in pollen and soil records. *The Holocene* 15, 263-277.

Dale, B., 1976. Cyst formation, sedimentation, and preservation: factors affecting dinoflagellate assemblages in recent sediments from Trondheimsfjord, Norway. *Review of Palaeobotany and Palynology* 22, 39-60.

Dale, B., 1996. Dinoflagellate cyst ecology: modelling and geological applications. In: Jansonius, J., McGregor, D. C. (Eds), *Palynology: Principles and Applications*. Vol. 3, American Association of Stratigraphic Palynologist, Salt Lake City, pp. 1249-1275.

Dale, B., Thorsen, T. A., Fjellså, A., 1999. Dinoflagellate cysts as indicators of cultural eutrophication in the Oslofjord, Norway. *Estuarine, Coastal and Shelf Science* 48, 371-382.

Daskalov, G. M., 2002. Overfishing drives a trophic cascade in the Black Sea. *Marine Ecology Progress Series* 225, 53-63.

Di Lorio, D., Yüce, H., 1999. Observations of Mediterranean flow into the Black Sea. *Journal of Geophysical Research* 104-C2, 3091-3108.

Eker-Develi, E., Kideys, A.E., 2003. Distribution of phytoplankton in the southern Black Sea in summer 1996, spring and autumn 1998. *Journal of marine Systems* 39, 203-211.

Ellegaard, M., Moestrup, Ø., 1999. Fine structure of the flagellar apparatus and morphological details of *Gymnodinium nolleri* sp. nov. (Dinophyceae), an unarmored dinoflagellate producing a microreticulate cyst. *Phycologia* 38(4), 289-300.

Fægri, K., Iversen, J., 1989. *Textbook of pollen analysis* (4th Edition). John Wiley and Sons, Chichester.

Fensome, R. A., Taylor, F. J. R., Norris, G., Sarjeant, W. A. S., Wharton, D. I., Williams, G. L., 1993. *A Classification of Living and Fossil Dinoflagellates*. American Museum of Natural History, *Micropaleontology* 7.

Filipova-Marinova, M., Bozilova, E., 2002. Palaeoecological conditions in the area of the prehistorical settlement in the Bay of Sozopol during the Eneolithic. *Phytologia Balcanica* 8(2), 133-143.

Filipova-Marinova, M., 2003. Postglacial vegetation dynamics in the coastal part of the Stransxa Mountains, Southeastern Bulgaria. In: Tonkov, S. (Ed), *Aspects of Palynology and Paleoecology*. Pensoft, Sofia-Moscow, pp. 213-231.

Filipova-Marinova, M., 2006. Late Pleistocene/Holocene dinoflagellate cyst assemblages from the Southwestern Black Sea shelf. In: Ognjanova-Rumenova, N., Manoylov, K. (Eds), *Advances in phycological studies*, pp. 267-281.

Filipova-Marinova, M., 2007. Archaeological and paleontological evidence of climate dynamics, sea-level change, and coastline migration in the Bulgarian sector of the Circum-Pontic region. In: Yanko-Hombach, V., Gilbert, A. S., Panin, N., Dolukhanov, P. M. (Eds), *The Black Sea Flood question: changes in coastlines, climate and human settlement*. Springer, Dordrecht, pp. 453-481.

Glebov, A. Y., Shel'ting, S. K., 2007. Sea-level changes and coastline migration in the Russian sector of the Black Sea: application to the Noah's flood hypothesis. In: Yanko-Hombach, V., Gilbert, A. S., Panin, N., Dolukhanov, P. M. (Eds), *The Black Sea Flood question: changes in coastlines, climate and human settlement*. Springer, Dordrecht, pp. 731-773.

Gómez, F., Boicenco, L., 2004. An annotated checklist of dinoflagellates in the Black Sea. *Hydrobiologia* 517(1-3), 43.

Grimm, E. C., 1987. CONISS: a FORTRAN 77 program for stratigraphical constrained cluster analysis by the method of incremental sum of squares. *Computers & Geosciences* 13(1), 13.

Head, M. J., 1996. Modern dinoflagellate cysts and their biological affinities. In: Jansonius, J., McGregor, D. C. (Eds), *Palynology: principles and applications*, vol.3. American Association of Stratigraphic Palynologists Foundation, Salt Lake City, pp. 1197-1248.

Head, M. J., Lewis, J., De Vernal, A., 2006. The cyst of the calcareous dinoflagellate *Scrippsiella trifida*: resolving the fossil record of its organic wall with that of *Alexandrium tamarense*. *Journal of Paleontology* 80(1), 1-18.

Hiscott, R. N., Aksu, A. E., Yaşar, D., Kaminski, M. A., Mudie, P. J., Kostylev, V. E., MacDonald, J. C., İşler, F. I., Lord, A. R., 2002. Deltas south of the Bosphorus Strait record persistent Black Sea outflow to the Marmara Sea since ~10 ka. *Marine Geology* 190(1-2), 261-282.

Hiscott, R.N., Flood, R.D., Aksu, A.E., Kinney, J., Yasar, D., 2006. Saline density-current channel created by Mediterranean inflow to the Black Sea through the Bosphorus Strait: morphology, history, and surface-current modification imaged by swath mapping and Huntex boomer profiles. Abstract, International Congress of Sedimentology, Fukuoka, Japan.

Hiscott, R. N., Aksu, A. E., Mudie, P. J., Kaminski, M. A., Abrajano, T., Yaşar, D., Rochon, A., 2007. The Marmara Sea Gateway since ~16 Ka: non-catastrophic causes of paleoceanographic events in the Black Sea at 8.4 and 7.15 ka. In: Yanko-Hombach, V., Gilbert, A. S., Panin, N., Dolukhanov, P. M. , *The Black Sea Flood*

Question: changes in coastlines, climate and human settlement. Dordrecht, Springer, pp. 89-117.

Hiscott, R. N., Aksu, A. E., Mudie, P. J., Marret, F., Abrajano, T., Kaminski, M. A., Evans, J., Çakiroğlu, A. I., Yaşar, D., in press. A gradual drowning of the southwestern Black Sea shelf: evidence for a progressive rather than abrupt Holocene reconnection with the eastern Mediterranean Sea through the Marmara Sea Gateway. *Quaternary International*.

Hopkins, J. A., McCarthy, F. M. G., 2002. Post-depositional palynomorph degradation in Quaternary shelf sediments: a laboratory experiment studying the effects of progressive oxidation. *Palynology* 26, 167-184.

Jones, G. A., 1993. Tales of Black Sea sedimentation, exploration and colonization. *AMS Pulse* 2(1), 1-5.

Kemp, P., 1980. *Encyclopedia of Ships and Seafaring*. Crown Publishers Inc, New York.

Khrishev, K.V., Georgiev, V., 1991. Regional washout in the Pleistocene–Holocene boundary in the western Black Sea depression. *Comptes rendus de l'Académie bulgare des Sciences*, 44(9), 69–71.

King, C., 2004. *The Black Sea: a History*. Oxford University Press, Oxford, pp. 65-71.

Kleijne, A., 1993. *Morphology, Taxonomy and Distribution of Extant Coccolithophorids (Calcareous Nannoplankton)*. Enchede, Drukkerij FEBA B.V.

Kouli, K., Brinkhuis, H., Dale, B., 2001. *Spiniferites cruciformis*: a fresh water dinoflagellate cyst? *Review of Palaeobotany and Palynology* 113(4), 273-286.

Latif, M. A., Özsoy, E., Salihoğlu, I., Gaines, A. F., Baştürk, Ö., Yılmaz, A., Tuğrul, S., 1992. Monitoring via direct measurements of the modes of mixing and transport of wastewater discharges into the Bosphorus underflow. Technical Report No 92-2, Middle East Technical University, Institute of Marine Sciences, 1-98.

Lericolais, G., Popescu, I., Guichard, F., Popescu S-M., Manolakakis, L., 2007. Water-level fluctuations in the Black Sea since the Last Glacial Maximum. In: Yanko-Hombach, V., Gilbert, A. S., Panin, N., Dolukhanov, P. M. , *The Black Sea Flood Question: changes in coastlines, climate and human settlement*. Dordrecht, Springer, pp. 437-452

Lewis, J., Hallett, R., 1997. *Lingulodinium polyedrum* (*Gonyaulax polyedra*) a blooming dinoflagellate. *Oceanography and Marine Biology; an Annual Review* 35, 97-161.

Major, C. O., 2002. Non-eustatic controls on sea-level change in semi-enclosed basins. PhD Thesis, Columbia University, New York.

Major, C. O., Goldstein, S. L., Ryan, W. B. F., Lericolais, G., Piotrowski, A. M., Hajdas, I., 2006. The co-evolution of Black Sea level and composition through the last deglaciation and its paleoclimatic significance. *Quaternary Science Reviews* 25(17-18), 2031.

Marret, F., 1993. Les effets de l'acétolyse sur les assemblages des kystes de dinoflagellés. *Palynosciences* 2, 267-272.

Marret, F., Leroy, S., Chalier, F., Gasse, F., 2004. New organic-walled dinoflagellate cysts from recent sediments of Central Asian seas. *Review of Palaeobotany and Palynology* 129(1-2), 1-20.

Mart, Y., Ryan, W., Çağatay, M. N., McHugh, C., Giosan, L., Vachtman, D., 2006. Evidence for intensive flow from the Bosphorus northwards during the early Holocene. *Geophysical Research Abstracts* 8, Sref-ID: 1607-7962/gra/EGU06-A-02572.

Matsuoka, K., 1999. Eutrophication process recorded in dinoflagellate cyst assemblages - a case of Yokohama Port, Tokyo Bay, Japan. *The Science of the Total Environment* 231, 17-35.

Matsuoka, K., Joyce, L. B., Kotani, Y., Matsuyama, Y., 2003. Modern dinoflagellate cysts in hypertrophic coastal waters of Tokyo Bay, Japan. *Journal of Plankton Research* 25(12), 1461-1470.

Mudie, P. J., Aksu, A. E., Yaşar, D., 2001. Late Quaternary dinoflagellate cysts from the Black, Marmara and Aegean seas: Variations in assemblages, morphology and paleosalinity. *Marine Micropaleontology* 43(1-2), 155.

Mudie, P. J., Rochon, A., Aksu, A. E., Gillespie, H., 2002. Dinoflagellate cysts, freshwater algae and fungal spores as salinity indicators in Late Quaternary cores from Marmara and Black seas. *Marine Geology* 190(1-2), 203.

Mudie, P. J., Rochon, A., Aksu, A. E., Gillespie, H., 2004. Late glacial, Holocene and modern dinoflagellate cyst assemblages in the Aegean-Marmara-Black Sea corridor:

Statistical analysis and re-interpretation of the early Holocene Noah's Flood hypothesis. *Review of Palaeobotany and Palynology* 128(1-2), 143.

Mudie, P. J., Marret, F., Aksu, A. E., Hiscott, R. N., Gillespie, H., in press.
Palynological evidence for climatic change, anthropogenic activity and outflow of Black Sea Water during the late Pleistocene and Holocene: centennial- to decadal-scale records from the Black and Marmara Seas. *Quaternary International*.

Murray, J. W., 1991. Hydrographic variability in the Black Sea. In: Izdar, E., Murray, J. W. (Eds), *Black Sea Oceanography*. NATO ASI Series, Series C: Mathematical and Physical Sciences V 351, Kluwer Academic Publishers, London, pp. 1-15.

Oğuz, T., 1993. Circulation in the surface and intermediate layers of the Black Sea. *Deep-Sea Research, Part I* 40(8), 1597.

Oğuz, T., 2005. Long-term impacts of anthropogenic forcing on the Black Sea ecosystem. *Oceanography* 18, 112-121.

Oğuz, T., Merico, A., 2006. Factors controlling the summer *Emiliania huxleyi* bloom in the Black Sea: A modeling study. *Journal of Marine Systems* 59(3-4), 173.

Özsoy, E., Latif, M. A., Tuğrul, S., Ünlüata, Ü., 1995. Exchanges with the Mediterranean, fluxes and boundary mixing processes in the Black Sea. In: Briand, F. (Ed), *Mediterranean Tributary Seas*. Bulletin de l'Institut Océanographique, Monaco, Special No 15. CIESME Science Series V 1, Monaco, pp. 1-25.

Özsoy, E., Latif, M. A., Sur, H. I., Goryachkin, Y., 1996. A review of the exchange flow regimes and mixing in the Bosphorus Strait. In: Briand F. (Ed.), *Mediterranean*

Tributary Seas. Bulletin de l'Institut Océanographique, Special No 17. CIESME Science Series V 2, Monaco, pp. 187-204.

Parker, A. J., 1973. Evidence provided by underwater archaeology for Roman trade in the western Mediterranean. In: Blackman, D. J. (Ed), Marine Archaeology. Butterworths, London, pp 361-379.

Polat, Ç., Tuğrul, S., 1996. Chemical exchange between the Mediterranean and Black Sea via the Turkish Straits. In: Briand, F. (Ed), Dynamics of Mediterranean Straits and Channels. Bulletin de l'Institut Océanographique, Special No 17. CIESME Science Series V 2, Monaco, pp. 167-186.

Ravazzi, C., 2006. Comment on "Paleoclimatic record of the past 22,000 years in Venice (Northern Italy): biostratigraphic evidence and chronology" by Serandrei Barbero et al. [Quaternary International 140-141, 37-52] "Interstadials" or phases of accumulation of reworked pollen? Quaternary International 148, 165-167.

Ross, D.A., Degens, E.T., 1974. Recent sediments of the Black Sea. In: Degens E.T. and Ross D.A. (Eds), The Black Sea: geology, chemistry, and biology. American Association Petroleum Geologists Memoirs 20, Tulsa, Oklahoma, pp. 183-199.

Ryan, W. B. F., Pitman, W. C., Major, C. O., Shimkus, K., Moskalenko, V., Jones, G. A., Dimitrov, P., Gorur, N., Sakinc, M., Yüce, H., 1997. An abrupt drowning of the Black Sea shelf. Marine Geology 138(1-2), 119-126.

Ryan, W. B. F., Major, C. O., Lericolais, G., Goldstein, S., 2003. Catastrophic flooding of the Black Sea. Annual reviews of Earth and Planetary Sciences 31, 525-554.

Ryan, W.B.F., 2007. Status of the Black Sea food hypothesis. In: Yanko-Hombach, V., Gilbert, A. S., Panin, N., Dolukhanov, P. M. , The Black Sea Flood Question: changes in coastlines, climate and human settlement. Dordrecht, Springer, pp. 63-88.

Severin, T., 1985. The Jason Voyage. Hutchinson & Co. Ltd, London.

Swiny, H. W., Katzev, M. L., 1973. The Kyrenia shipwreck: a fourth-century B.C. In: Blackman, D. J. (Ed), Marine Archaeology. Butterworths, London, pp. 339-355.

Thorsen, T. A., Dale, B., Nordberg, K., 1995. 'Blooms' of the toxic dinoflagellate *Gymnodinium catenatum* as evidence of climatic fluctuations in the late Holocene of southwestern Scandinavia. The Holocene 5(4), 435-446.

Torr, C., 1964. Ancient Ships. Argonaut Inc, Chicago.

UNESCO, 1969. Discharge of Selected Rivers of the World, Vol. 1: General and Regime Characteristics of Stations Selected. Studies and Reports in Hydrology, 1-70.

UNESCO, 1993. Discharge of Selected Rivers of the World, Vol. 2: Monthly and Annual Discharges Recorded at Various Selected Station. Studies and Reports in Hydrology, 1-600.

Wall, D., Dale, B., 1973. Palaeosalinity relationships of dinoflagellates in the late Quaternary of the Black Sea - A summary. Geosciences Man VII, 95-102.

Wall, D., Dale, B., Harada, K., 1973. Description of new fossil dinoflagellates from the Late Quaternary of the Black Sea. *Micropaleontology* 19(1), 18-31.

Winter, A., Jordan, R. W., Roth, P. H., 1994. Biogeography of the living coccolithophores in the oceans. In: Winter, A., Siesser, W. (Ed), *Coccolithophores*. Cambridge University Press, pp. 161-178.

Yanko-Hombach, V., Gilbert, A. S., Panin, N., Dolukhanov, P. M. (Eds), 2007. *The Black Sea flood question: Changes in coastline, climate and human settlement*. Springer, Dordrecht.

Figure caption

Figure 1: A) Map of core sites cited in Table 1 with bathymetry (except for the Caspian Sea). Black rectangle is core M02-45. B) Detailed bathymetry for the BS southwestern shelf.

Figure 2: Huntec deep tow system boomer profile showing the three seismic units 1B, 1C and 1D at the core site M02-45. Note that unit 1D subtly onlaps unit 1C toward the NE,

Figure 2: Percentage diagram of all dinocyst and freshwater taxa versus depth. The stratigraphic log is depicted on the left-side of the diagram. Zonations were established with the cluster analysis (CONISS, TILIA).

Figure 3: Percentage diagram of selected taxa and fluxes versus age (radiocarbon uncalibrated ka, uncorrected for reservoir effect).

Plate caption

Plate 1

All micrographs were taken on a light-transmitted microscope. Scale bar is 10µm.

1- Cysts of *Gymnodinium catenatum/nolleri*, core depth 50 cm.

2- Cyst of *G. catenatum/nolleri*, core depth 130 cm

3- *Echinidinium transparantum*, core depth 130 cm

4- *E. transparantum*, core depth 180cm

5- Cyst of *Polykrikos kofoidii*, core depth 150 cm

6- *Islandinium minutum*, core depth 150 cm

7- *Dubridinium caperatum*, core depth 300 cm

8- Cyst of *Protoperidinium stellatum*, core depth 70 cm

9- *Peridinium ponticum*, dorsal view, core depth 150 cm

10- *P. ponticum*, apical view, core depth 150 cm

11- *Quinquecuspis concreta*, dorsal view, core depth 330 cm

12- *Lingulodinium machaerophorum sensu stricto*, dorsal view, core depth 470 cm

13- *L. machaerophorum* with short and bulbous processes, core depth 360 cm

14- *Spiniferites belerius*, dorsal view, core depth 430 cm

15- *Spiniferites bentorii*, optical view, core depth 440 cm

16- *Spiniferites* cf. *belerius* with weak cruciform body shape, optical view, core depth 470 cm

17- *S.* cf. *belerius* with pronounced cruciform body shape, ventral view, core depth 440 cm

18- *S.* cf. *belerius* with pronounced cruciform body shape and apical node, optical view, core depth 430 cm

19- *Spiniferites cruciformis* with relatively short processes, dorsal view, core depth 940 cm

20- *S. cruciformis* with ventral fringe, dorsal view, core depth 530 cm

21- *S. cruciformis* sensu Wall et Dale in Wall et al., 1973, dorsal view, core depth 550 cm

22- *Pyxidinosia psilata* with vermiculate ornamentation, dorsal view, core depth 580 cm

23- *P. psilata* with smooth wall surface, dorsal view, core depth 550cm

24- *Botryococcus* sp., core depth 590 cm

Table 1: Late Pleistocene and Holocene dinocyst records from the Marmara and Black Sea (see *Figure 1* for the location of the cores). Location of core-tops from the Caspian Sea are indicated with a dot (see Marret *et al.*, 2004).

| Site number | Region | References |
|--------------------|--|---|
| 1-5 | Marmara Sea, southwestern and southeastern Black Sea | Mudie <i>et al.</i> , (2002, 2004) |
| 6-8 | East and west Black Sea | Wall and Dale (1973); Wall <i>et al.</i> (1973) |
| 9-11 | Southwestern and Western Black Sea | Filipova-Marinova and Bozilova (2002); Filipova-Marinova (2003, 2006, 2007) |
| 12-21 | Western Black Sea | Atanassova and Bozilova, (1992); Atanassova (1995, 2005) |
| 22 | Southwestern Black Sea | This study |

Table 2: Radiocarbon ages reported as uncalibrated conventional ^{14}C dates in yr BP (half-life of 5568 years; errors represents 68.3% confidence limits) and uncorrected for the reservoir effect. Analyses carried out by the IsoTrace Radiocarbon Laboratory, Accelerator Mass Spectrometry Facility, University of Toronto.

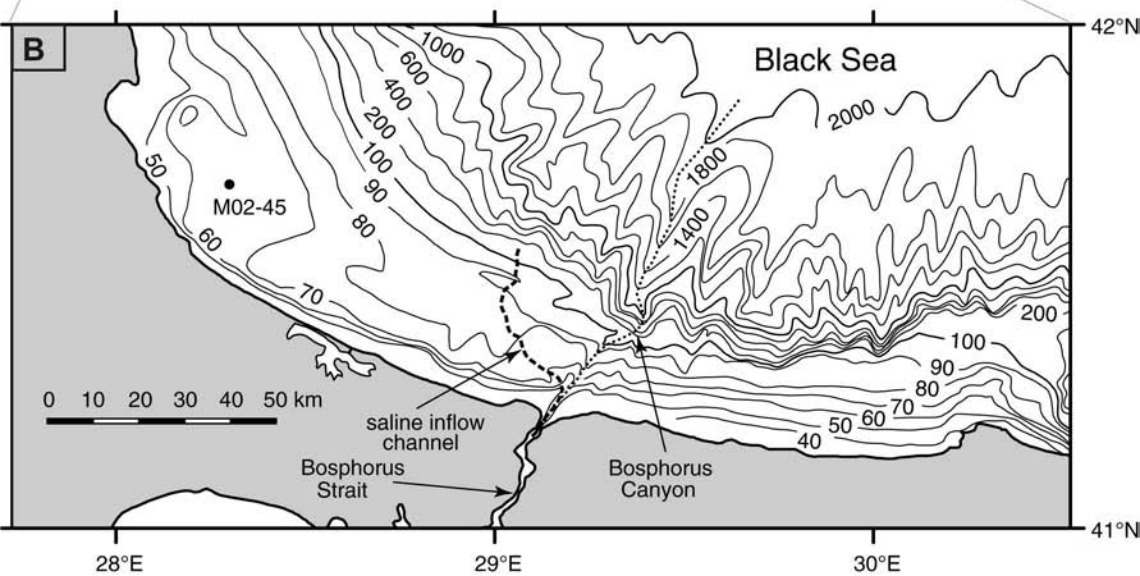
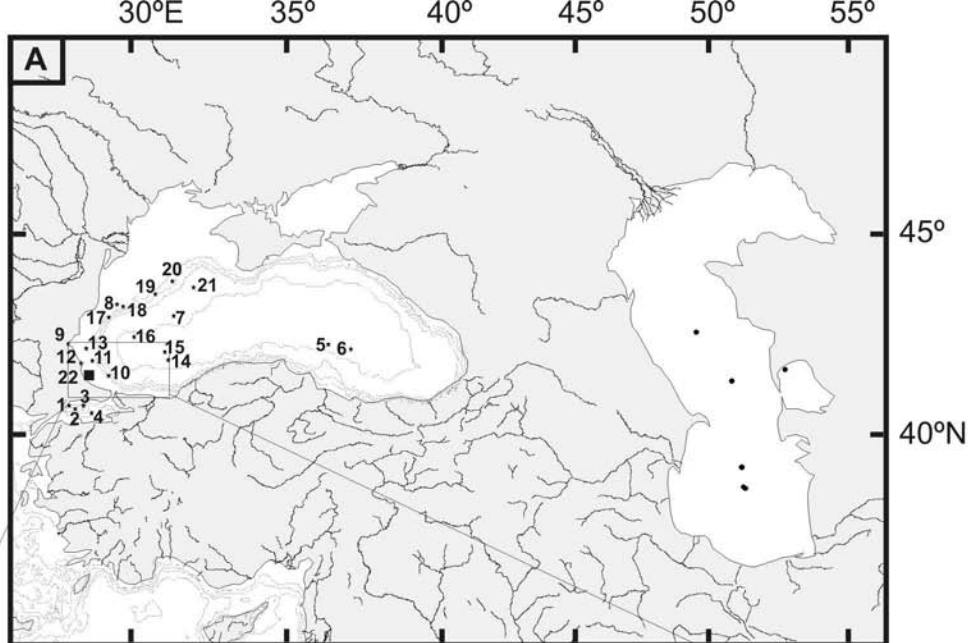
| Core Number | Depth (cm) | Material dated | Age (yr BP) | IsoTrace Number |
|--------------------|-------------------|----------------------------------|--------------------|------------------------|
| MAR 02-45T | 92 | <i>Spisula subtruncata</i> | 730±50 | TO-11433 |
| MAR 02-45T | 145 | <i>Spisula subtruncata</i> | 770±50 | TO-11434 |
| MAR 02-45P | 33 | <i>Spisula subtruncata</i> | 730±40 | TO-11435 |
| MAR 02-45P | 158 | <i>Mytilus edulis</i> | 2400±60 | TO-11006 |
| MAR 02-45P | 220 | <i>Mytilus edulis</i> | 5190±50 | TO-11436 |
| MAR 02-45P | 302 | <i>Mytilus galloprovincialis</i> | 5900±60 | TO-11437 |
| MAR 02-45P | 406 | <i>Anadara</i> spp. | 7560±60 | TO-11438 |
| MAR 02-45P | 495 | <i>Truncatella subcylindrica</i> | 8380±70 | TO-11142 |
| MAR 02-45P | 569 | <i>Anadara</i> spp. | 8570±70 | TO-11439 |
| MAR 02-45P | 639 | <i>Anadara</i> spp. | 8620±70 | TO-11440 |
| MAR 02-45P | 754 | <i>Dreissena polymorpha</i> | 8840±70 | TO-11441 |
| MAR 02-45P | 810 | <i>Mytilus edulis</i> | 9370±70 | TO-11007 |
| MAR 02-45P | 822 | <i>Dreissena polymorpha</i> | 9340±70 | TO-11442 |
| MAR 02-45P | 835 | <i>Cyclope donovani</i> | 9070±70 | TO-11443 |

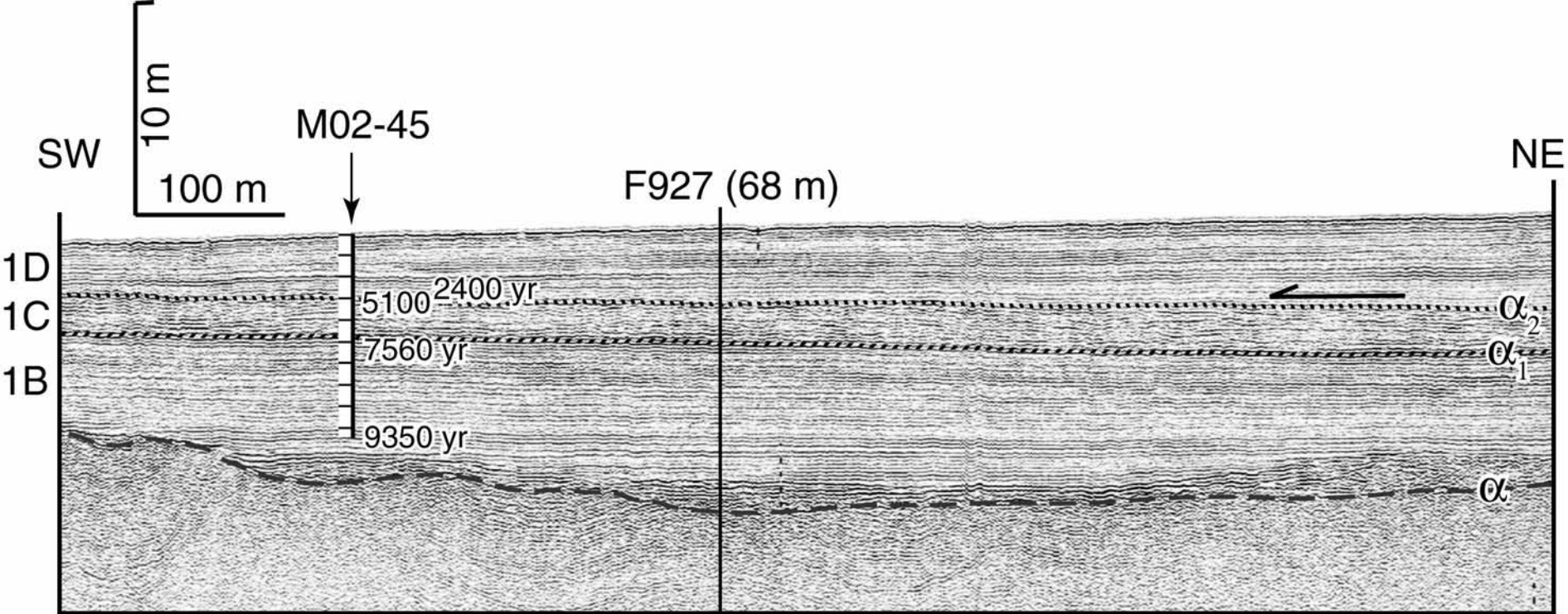
Table 3: List of identified dinoflagellate cyst taxa in core M0245. Legend for their modern occurrence: O: Oceans, BS: Black Sea, CS: Caspian Sea, AS: Aral Sea, LZ: Lake Zürich, BaS: Baltic Sea. * indicates motile stage occurring in the Black Sea at present (Gómez and Boicenco, 2004)

| Cyst name | Modern occurrence | Thecate affinity |
|--|-------------------|--------------------------------------|
| Gonyaulacaceae | | |
| <i>Caspidinium rugosum</i> | CS | unknown |
| Cysts of <i>Gonyaulax apiculata</i> | LZ | ? <i>Gonyaulax apiculata</i> * |
| <i>Impagidinium caspiensis</i> | CS, AS | unknown |
| <i>Lingulodinium machaerophorum</i> and morphotypes | O | <i>Lingulodinium polyedrum</i> * |
| <i>Operculodinium centrocarpum</i> sensu Wall & Dale | O | <i>Protoceratium reticulatum</i> * |
| <i>Pyxidinosopsis psilata</i> | CS, BaS | unknown |
| <i>Polysphaeridium zoharyi</i> | O | <i>Pyrodinium bahamense</i> |
| <i>Spiniferites belerius</i> | O | <i>Gonyaulax scrippsae</i> * |
| <i>Spiniferites</i> cf. <i>belerius</i> | O | ? <i>Gonyaulax scrippsae</i> * |
| <i>Spiniferites bentorii</i> | O | <i>Gonyaulax digitale</i> * |
| <i>Spiniferites</i> cf. <i>bentorii</i> | O | ? <i>Gonyaulax digitale</i> * |
| <i>Spiniferites bulloideus</i> | O | <i>Gonyaulax scrippsae</i> * |
| <i>Spiniferites cruciformis</i> and morphotypes | CS, AS | unknown |
| <i>Spiniferites inaequalis</i> | | unknown |
| <i>Spiniferites membranaceus</i> | O | <i>Gonyaulax membranacea</i> * |
| <i>Spiniferites mirabilis</i> | O | <i>Gonyaulax spinifera</i> group* |
| <i>Spiniferites ramosus</i> | O | <i>Gonyaulax</i> sp. |
| <i>Spiniferites</i> spp. | O | <i>Gonyaulax</i> sp. |
| <i>Tectatodinium pellitum</i> | O | <i>Gonyaulax spinifera</i> group* |
| Peridiniaceae | | |
| Cyst of <i>Pentapharsodinium dalei</i> | O | <i>Pentapharsodinium dalei</i> |
| Proto-peridiniaceae | | |
| <i>Brigantedinium</i> spp. | O | <i>Proto-peridinium</i> sp. |
| <i>Brigantedinium simplex</i> | O | <i>Proto-peridinium conicoides</i> * |
| <i>Dubridinium caperatum</i> | O | <i>Preperidinium meunieri</i> * |
| <i>Echinidinium transparentum</i> | O | unknown |
| <i>Echinidinium</i> spp. | O | unknown |
| <i>Islandinium minutum</i> | O | ? <i>Proto-peridinium</i> sp. |
| <i>Lejeunecysta oliva</i> | O | ? <i>Proto-peridinium</i> sp. |
| <i>Peridinium ponticum</i> | BS | ? <i>Proto-peridinium</i> sp. |
| <i>Proto-peridinium</i> sp. A | | Unknown |
| Cysts of <i>Proto-peridinium stellatum</i> | O | <i>Proto-peridinium stellatum</i> |
| <i>Quiquecuspis concreta</i> | O | ? <i>Proto-peridinium leonis</i> * |
| <i>Selenopemphix nephroides</i> | O | <i>Proto-peridinium subinermis</i> * |
| <i>Votadinium calvum</i> | O | <i>Proto-peridinium oblongum</i> * |
| <i>Votadinium spinosum</i> | O | <i>Proto-peridinium claudicans</i> * |
| <i>Xandarodinium xanthum</i> | O | <i>Proto-peridinium divaricatum</i> |
| Polykrikaceae | | |
| Cysts of <i>Polykrikos kofoidii</i> | O | <i>Polykrikos kofoidii</i> * |
| Gymnodiniaceae | | |
| Cyst of <i>Gymnodinium catenatum/nolleri</i> | O | <i>Gymnodinium catenatum/nolleri</i> |

Table 4: Synthesised dinocyst record for the Holocene of the Black Sea. Data are compiled from Table 1 and the present study. Note that dinocyst percentages from sites 9 to 21 were calculated based on a sum of pollen + dinocysts, which may have hindered some significant changes.

| Age ka BP | Sites 1-5 | Sites 6-8 | Sites 9-11 | Sites 12-21 | M02-45 |
|-----------|--|--|--|---|---|
| 0 | <i>L. machaerophorum</i> <i>Spiniferites</i> spp. <i>O. centrocarpum</i> | <i>L. machaerophorum</i> <i>P. ponticum</i> | <i>L. machaerophorum</i> <i>S. ramosus</i> <i>Peridinium</i> | <i>L. machaerophorum</i> <i>Spiniferites</i> spp. <i>Cymatiosphaera</i> | <i>L. machaerophorum</i> <i>O. centrocarpum</i> <i>Spiniferites</i> spp. <i>G. catenatum/nolleri</i> <i>P. ponticum</i> ----- <i>L. machaerophorum</i> and morphotypes + <i>S. belerius</i> and <i>S. bentorii</i> morphotypes ----- <i>P. psilata</i> , <i>S. cruciformis</i> Small occurrence of <i>L. machaerophorum</i> <i>Spiniferites</i> spp., <i>Brigantedinium</i> spp., <i>Pediastrum</i> , <i>Botryococcus</i> |
| 1 | | <i>L. machaerophorum</i> | ----- | | |
| 2 | | | <i>L. machaerophorum</i> | | |
| 3 | | <i>Cymatiosphaera</i> | | | |
| 4 | | | | | |
| 5 | | <i>Cymatiosphaera</i> | | | |
| 6 | <i>Cymatiosphaera</i> | | | | |
| 7 | <i>P. psilata</i> <i>S. cruciformis</i> <i>G. apiculata</i> <i>Peridinium</i> sp. | <i>P. psilata</i> <i>S. cruciformis</i> | ~6.8 ka BP | <i>P. psilata</i> <i>S. cruciformis</i> Small occurrence of <i>L. machaerophorum</i> and <i>Spiniferites</i> spp. | ----- |
| 8 | | | | | |
| 9 | | | | | |
| 10 | | | | | |
| 11 | | | | | |
| 12 | | | | | |
| 13 | | | | | |
| 14 | | | | | |
| | Diversity ~ 19 | Diversity~12 | Diversity ~6 | Diversity ~ 4 | Diversity ~32 |





MAR02-45

